AIP | The Journal of Chemical Physics

Local order of liquid water at metallic electrode surfaces

Luana S. Pedroza, Adrien Poissier, and M.-V. Fernández-Serra

Citation: The Journal of Chemical Physics **142**, 034706 (2015); doi: 10.1063/1.4905493
View online: http://dx.doi.org/10.1063/1.4905493
View Table of Contents: http://scitation.aip.org/content/aip/journal/jcp/142/3?ver=pdfcov
Published by the AIP Publishing

Local order of liquid water at metallic electrode surfaces

Luana S. Pedroza,[1] Adrien Poissier,[1] and M.-V. Fernández-Serra[1,2,a)]
[1]*Department of Physics and Astronomy, Stony Brook University, Stony Brook, New York 11794-3800, USA*
[2]*Institute for Advanced Computational Sciences, Stony Brook University, Stony Brook, New York 11794-3800, USA*

(Received 20 August 2014; accepted 19 December 2014; published online 21 January 2015)

We study the structure and dynamics of liquid water in contact with Pd and Au (111) surfaces using *ab initio* molecular dynamics simulations with and without van der Waals interactions. Our results show that the structure of water at the interface of these two metals is very different. For Pd, we observe the formation of two different domains of preferred orientations, with opposite net interfacial dipoles. One of these two domains has a large degree of in-plane hexagonal order. For Au, a single domain exists with no in-plane order. For both metals, the structure of liquid water at the interface is strongly dependent on the use of dispersion forces. The origin of the structural domains observed in Pd is associated to the interplay between water/water and water/metal interactions. This effect is strongly dependent on the charge transfer that occurs at the interface and which is not modeled by current state of the art semi-empirical force fields. © *2015 AIP Publishing LLC.* [http://dx.doi.org/10.1063/1.4905493]

I. INTRODUCTION

In the last few years, there has been an explosion of fundamental physics research in the field of electrochemical energy conversion or storage, driven by the need of optimizing and discovering new materials for renewable energy applications, such as photo-electrochemical fuel cells.[1–3] While both experimental and theoretical surface scientists have made a lot of progress on the understanding and characterization of both atomistic structures and reactions at the solid/vacuum interface,[4–14] the theoretical description of electrochemical interfaces is still lacking behind. A reason for this is that a complete and accurate first principles' description of both the liquid and the metal interfaces is still computationally too expensive and complex, since their characteristics are governed by the explicit atomic and electronic structure built at the interface as a response to environmental conditions. Therefore, most studies to date have studied the fully solvated electrochemical interface using only a classical or semiclassical description. Fully first principles studies have simulated one[9,10] or two[13,14] bilayers of ordered or semi-ordered water or liquid water structures obtained from classical molecular dynamics simulations in contact with metal electrodes.[3,15] Izvekov *et al.*[16,17] performed short first principle simulations of Ag and Cu-water interface, and more recently, the interface Au-water has been analyzed.[18,19] However, the question of what is the actual structure of pure liquid water at the metal electrode interface is still an open one for most of the metals. This is a critical first step to validate current models of the electrochemical, i.e., ionic aqueous solution/metal, interface.[20–23]

In this work, we overcome the limitation of classical potentials and analyze in detail, the structure and interfacial charge redistribution of liquid-water interacting with Pd and Au (111) surfaces at ambient temperature, using first principles molecular dynamics. The study will reveal that, contrary to what was found when studying ice-like water overlayers,[10,24] long range dispersion (van der Waals, vdW) interactions play a critical role in modeling the aqueous/electrode interface and results are very different to those obtained when vdW interactions are not accounted for.

II. METHODOLOGY

We perform DFT-based *Ab Initio* molecular dynamics (AIMD) using the Siesta code.[25,26] Two different exchange and correlation (XC) functionals are used in this study. One is the PBE (Perdew-Burke-Ernzerhof)[27] gradient-corrected (GGA) functional, which in the past has been the standard functional choice for water/metal studies.[10,24] We also perform simulations with a modified version of the vdW functional proposed by Dion *et al.*[28] (DRSLL), in which PBE is used as the local term of DRSLL functional, instead of revPBE as originally proposed. This vdW-DF^{PBE} functional has recently been shown to produce good dynamical and structural properties of liquid water.[29,30]

For Pd(111) surfaces, the unit cell consists of 4 layers of 24 Pd atoms (96 in total) and 80 H_2O molecules, with size 9.715 $\times$ 16.826 $\times$ 26.968 Å. This choice reflects the need of having a unit cell large enough in all directions to ensure the correct treatment of liquid water. No k-points were sampled, but the in plane unit cell dimensions ensure an effective sampling of 24-k points.[7] Norm-conserving pseudopotentials in the Troullier-Martins form[31] are used to describe core electrons, both for metal and water. The valence electrons are described using a variationally optimized basis set of numerical atomic orbitals with double-ζ polarized (DZP) size. More details on the basis sets can be found in Refs. 7 and 32. As it was shown in Ref. 33, this water DZP basis set does not compromise the sampling of

a)Author to whom correspondence should be addressed. Electronic mail: maria.fernandez-serra@stonybrook.edu

configuration space explored in the AIMD, giving negligible errors in ionic forces when compared to bigger basis set and to plane waves calculations.

Periodic boundary conditions ensure that water is confined at a fixed (experimental) density and in contact with the two sides of the metal slab. Therefore, two interfaces are formed in each AIMD. This choice reflects the need of performing comparisons of XC functionals at constant density instead of having a metal/water/vacuum structure in which the large differences between equilibrium density of the different functionals would significantly affect the metal/water interface.[29] To evaluate the importance of sampling, and of the initial configuration, we have performed two distinct simulations with different initial conditions for the water molecules. This sampling part of our study is only done for the PBE simulations, although short simulations using vdW-DF^{PBE} provide the same qualitative conclusions. In one simulation, two 2-D monolayers of ice of 16 water molecules each were adsorbed at each side of the Pd-(111) slab. 48 additional liquid water molecules were inserted in the remaining space between the two Pd surfaces. The second one contained the same total number of H_2O molecules (80), all of them in liquid form, inserted between the two metallic slabs. In both cases, liquid water has been first equilibrated by a classical molecular dynamics for 20 ps. The motivation behind this choice was to test whether the well characterized 2-D ice bilayer[10,24] would retain certain amount of order, or even induce some additional order when the metal surface is fully wet with liquid water at room temperature. While a previous work[14] has studied the stability of up to two 2-D ice bilayers in different metals, no study has yet considered their stability in fully solvated conditions at room temperature T for Pd. All our production runs are at least 10 ps long, with a time step of 0.5 fs. They are performed in the micro-canonical ensemble and followed an AIMD annealing run to $T = 325$ K for PBE and $T = 300$ K for vdW-DF^{PBE} during 5 ps. Our results show that the different initial conditions do not appear to affect the final interfacial water structures, the results being qualitatively similar for both cases (as shown in Fig. 1), indicating that 10 ps are enough to achieve the formation of a converged interfacial water structure. Indeed, in all our simulations, the interfacial structure formed within 2 ps, after the initial 5 ps pre-equilibration period. Details of all the simulations performed are presented in Table I.

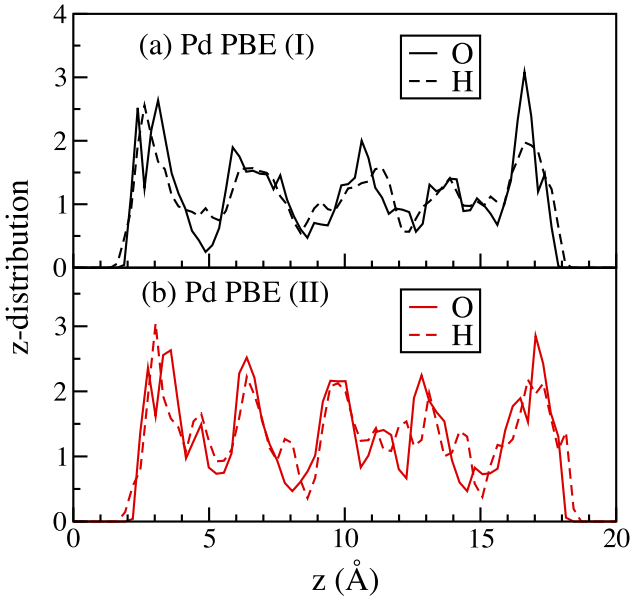

FIG. 1. z-distribution of O and H computed along the z–distance (in Å) for the Pd/H_2O (PBE) simulations starting from two different initial conditions. The position of the last layer of atoms at the Pd(111) surface is set to zero and to 20 Å. In (a), we had the same total number of H_2O molecules (80), all of them in liquid form inserted between the two metallic slabs. In (b), two 2-D monolayers of ice of 16 water molecules each were adsorbed at each side of the Pd-(111) slab. 48 additional liquid water molecules were inserted in the remaining space between the two Pd surfaces.

III. RESULTS

A. Structure of interfacial water: Pd(111)

In Figs. 2(a) and 2(c), we show the distribution of O and H atoms at a given z distance from the surface at the two interfaces for both PBE and vdW-DF^{PBE}, respectively. The position of the last Pd(111) layer of atoms at the Pd(111) surface is set to zero in z for both sides of the slab.

For PBE, the interface in the upper plot of Fig. 2(a) presents a sharp double peak for the O atoms. The peak closer to the surface originates from molecules adsorbed in a "flat" geometry, i.e., the molecule's dipole moment is mostly parallel to the surface. In a standard monolayer of ice on top of a ⟨111⟩ metallic surface, flat water molecules tend to be closer to the surface compared to the up(down) ones by around 0.5 Å. The second peak is due to the "up/down" molecules, which donate one H-bond to a flat molecule and the other to a molecule in a layer above ("up") or to the metal ("down"). The maximum of probability to find H at the left interface occurs between the two oxygen peaks, corresponding to the H-bond within the interfacial layer. The other interface, shown at the bottom of Fig. 2(a), presents a smaller peak related to the presence of flat molecules close to the surface and a broad peak composed of mostly "down" molecules. Down water molecules can be seen as the tail of H probability that is closer to the surface than to O, at both interfaces. Therefore, on average, water molecules from this interface (bottom) are further away from the metal than the molecules on the other interface (top). In this case, there is little in-plane order, with a structure very similar to what is shown in Fig. 2(d). We refer to this as a "disordered" domain. The complete z-distribution profiles for the PBE simulations are shown in Fig. 1. Fig. 2(b) shows the probability of finding an atom at a particular position on the XY plane, integrated over the first layer and averaged over all the simulation length. The first layer is defined by the first minimum of the O-atoms in the z-distribution profile and corresponds to ∼4.4 Å, for all simulations. The hexagonal lattice of surface Pd atoms is shown in black small spots. Oxygen atoms are shown in red and H atoms in blue. The figure shows the formation of an ordered domain of hexagons and pentagons, with very stable flat molecules, that are represented by the double peak in the z-distribution (upper plot of Fig. 2(a)). This structural asymmetry is formed at the very beginning of PBE simulation (∼1.5 ps) and remains stable for the remaining of it. Moreover, the asymmetry is independent of the initial conditions and has also occurred

TABLE I. Details of the simulations performed for the water/metal systems. We show the exchange-correlation functional (E_{xc}) used, total charge of the system (charge), the number of water molecules (H_2O), the number of metal layers per unit cell (metal layers), the number of metal atoms per layer (metal atoms), the unit cell size in Å (cell), the time of simulation after equilibration in ps (time) and the temperature T (K). For Pd, the lattice parameter is 3.96 Å and for Au it is 4.02 Å. All simulations started with the initial condition described in Fig. 1(a), except the one marked with (*) that started considering two 2-D monolayers of ice adsorbed (Fig. 1(b)).

System	E_{xc}	Charge (e)	H_2O	Metal layers	Metal atoms	Cell (Å)	Time (ps)	T (K)
Pd/H_2O	PBE	0	80	4	24	$9.715 \times 16.826 \times 26.968$	10	325
Pd/H_2O(*)	PBE	0	80	4	24	$9.715 \times 16.826 \times 26.968$	10	325
Pd/H_2O	vdW-DF^{PBE}	0	80	4	24	$9.715 \times 16.826 \times 26.968$	10	300
Pd/H_2O	PBE	+1	80	4	24	$9.715 \times 16.826 \times 26.968$	10	325
Pd/H_2O	PBE	−1	80	4	24	$9.715 \times 16.826 \times 26.968$	10	325
Au/H_2O	PBE	0	37	4	12	$9.754 \times 9.373 \times 27.3008$	10	325
Au/H_2O	vdW-DF^{PBE}	0	37	4	12	$9.754 \times 9.373 \times 27.3008$	5	300

for some short simulations with different water densities. We have studied the binding energy of these two types of liquid interfaces with the Pd slab. The binding energy is per water molecule at the interface (i.e., not divided by the total number of water molecules, but only for the molecules at the interface). We define this binding energy to be $E_b = \frac{1}{2}E(W_iPdW_j) - E(W_i) - E(W_j) - E(Pd)$, where $W_{i,j}$ represents interfacial water type A ("ordered" domain) or B ("disordered" domain) and W_iPdW_j is a slab of vacuum/water/Pd/water/vacuum with symmetric (A/Pd/A, B/Pd/B) and asymmetric (A/Pd/B) interfaces. We do this for a series of 50 entirely randomly chosen snapshots along the simulation. Our results show that (i) symmetric interfaces are almost identical in energy ($E_b = 0.13 \pm 0.86$ eV/H_2O) and (ii) the asymmetric interface is the most stable ($E_b = 0.15 \pm 0.41$ eV/H_2O). The large error bar for the binding energy is due the number of configurations considered. However, we have checked that the results are also converged for different numbers of water layers considered and with two times more Pd layers, revealing the trend of the asymmetric interface being more stable for the PBE functional.

When the simulation is repeated using vdW-DF^{PBE}, the interfacial order changes substantially. The double peak in the distribution profile is not well defined at any interface, as shown in Fig. 2(c). Flat orientations, which are driven by donor-covalent, H-bond type interactions between one of the O lone pairs and the metal,[5,7] are less favored when vdW

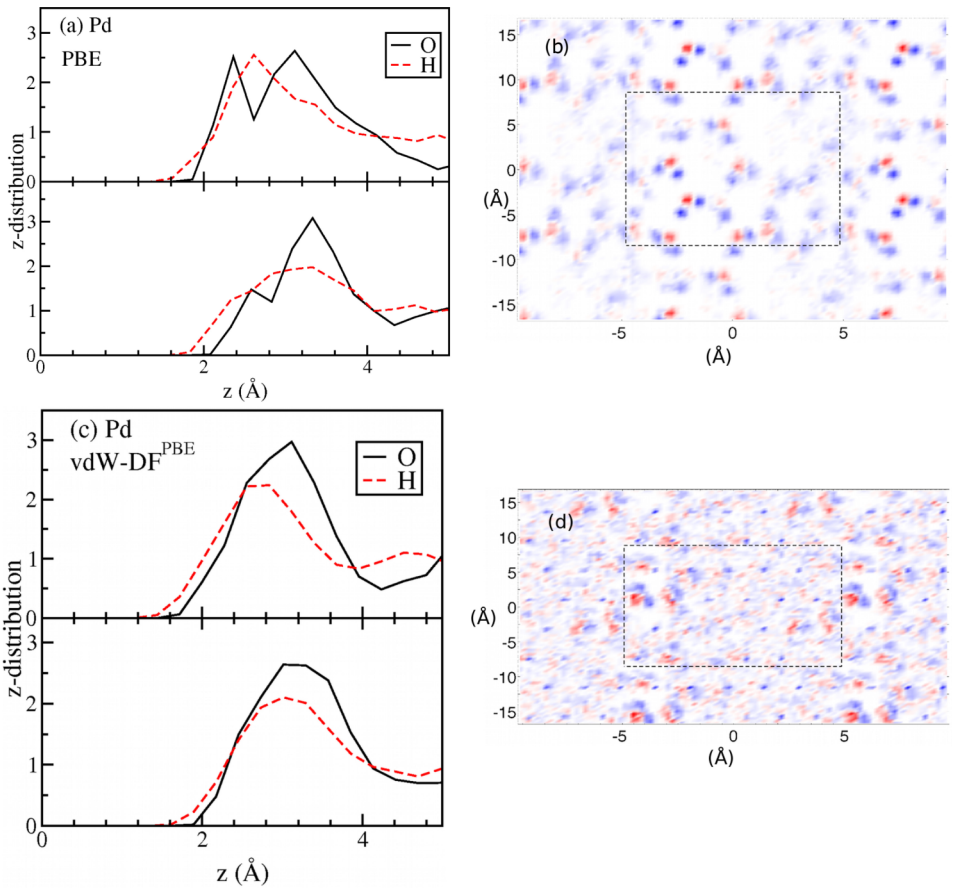

FIG. 2. z-distribution for O and H atoms computed along the z–distance (in Å) at the two Pd/H_2O interfaces for (a) PBE and (c) vdW-DF^{PBE}. The position of the last layer of atoms at the Pd(111) surface is set to zero in z for both sides of the slab. The XY surface probability at the interfaces is shown in (b) for PBE and in (d) for vdW-DF^{PBE}. Water molecules can be seen formed by O (red) and H (blue). The first Pd layer below is shown in small black spots. The square indicates the unit cell used in the AIMD simulations.

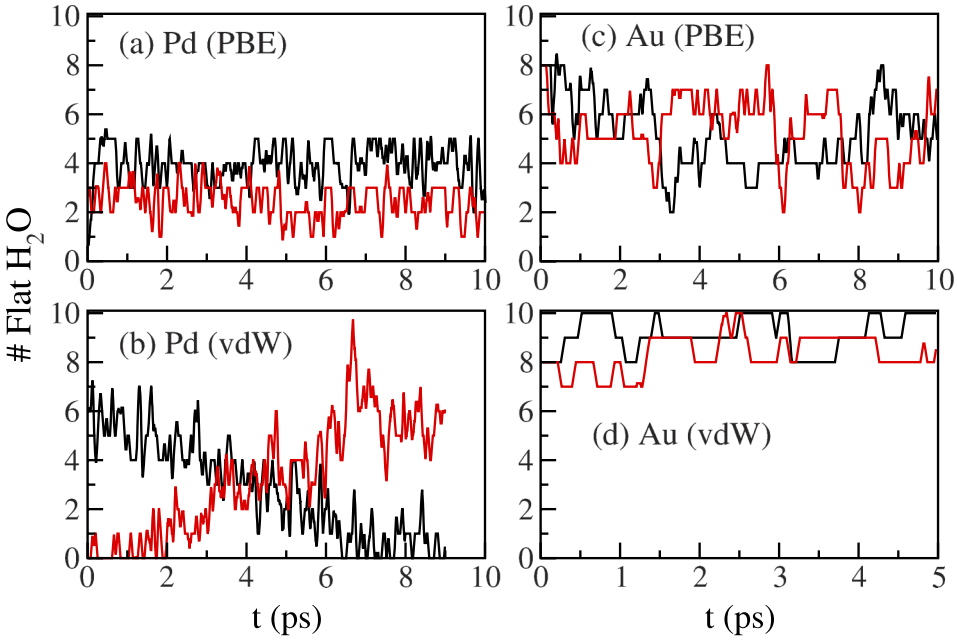

FIG. 3. Number of flat H_2O molecules at both metal interfaces for PBE (top panels) and vdW-DF^{PBE} (bottom panels) functionals: (a) and (b) for Pd(111) simulations and (c) and (d) for Au(111). Red and black represent the two interfaces, and only the water molecules at the interface were considered.

interactions are accounted for. These tend to favor more perpendicular orientations, which are also favored by dipole-image-dipole electrostatic interactions.[7,34] Indeed, the interfacial profiles in Fig. 2 are integrated for the full simulation length. A time dependent analysis of these profiles reveals that the water layers at the interfaces in the vdW simulation fluctuate between the previously described ordered and disordered domains, as can be seen in Fig. 3 which shows how the number of flat water molecules at both interfaces varies during the simulation (after the equilibration time). This number was defined by the number of molecules closer to the metal, i.e., distance O-metal less than ~2 Å. In Fig. 3, red and black represent the two interfaces due to the periodic boundary conditions. At any particular time, there is always an asymmetric interfacial configuration (Fig. 3(b)), resulting in a more disordered structure on average, as shown in Fig. 2(d), whereas in Fig. 3(a), the number of flat molecules in each side does not vary much.

The distinction of flat and up/down molecules can also be observed in Fig. 4, in which we show the angle distribution for the interfacial water molecules (using the same criteria as previously mentioned). The angle φ is defined as the angle between the vector normal to the plane of the water molecule and the vector normal to the metal surface. Therefore, when the molecule is fully flat this angle is 0°, and when it is perpendicular to the surface the angle is 90°. In Fig. 4(a) (Pd PBE), we can see that there are two peaks, corresponding to the flat and up/down molecules, as opposed to Fig. 4(b) (Pd vdW-DF^{PBE}), where the distribution is broader and it is more difficult to identify the different types of orientations. This is expected when we have a situation in which there is a dynamical transition in between the two types of domains, as shown in Fig. 3(b).

Depending upon the orientation of the water molecule towards the surface the metal may screen a negative or positive

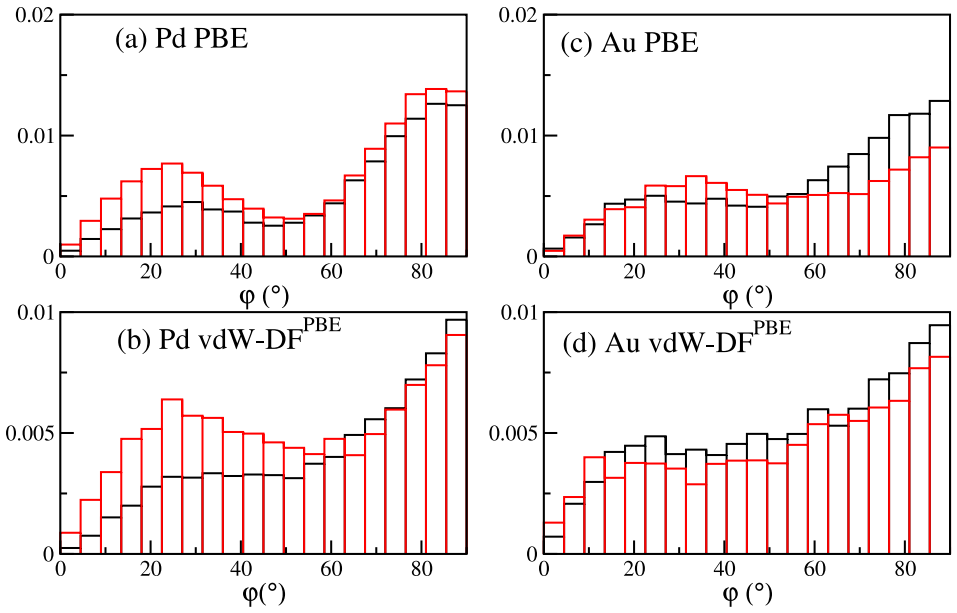

FIG. 4. Distribution of the angle between the vector normal to the plane of the water molecule and the vector normal to the metal surface. The φ angle distribution for the interfacial water molecules is plotted in black and red for the two interfaces.

charge. When the O atom is oriented towards the surface, it induces a positive image charge near the metal surface. When the molecular orientation has the H atom facing the metal, the opposite occurs and a negative image charge is induced. Besides this screening effect, the donor-covalent type of bond between flat molecules and the metal results in a charge transfer from the water molecules to metal.[7] We can then associate to regions with more flat molecules a domain where the surface will be more positively charged. And, contrary, a negative domain for regions where there is a presence of more molecules with hydrogen pointing down. The idea of charged domains has been shown before for water monolayers.[35] We can compute the net water to metal charge transfer per configuration by integrating the charge density difference between the solvated metal and the metal and water regions isolated. The results shown in Table II are an average over 20 representative configurations from the AIMD simulation. The size of the domains (and therefore the number of water molecules) is determined by the first minimum of the z-density. Our main conclusions are not affected by small deviations of this boundary. Assuming that most of this charge is transferred by "flat" molecules,[7] we estimate that for PBE the ordered domain shows a net 0.004 $e^-/\text{Å}^2$ charge loss to the metal. The disordered domain transfers only 0.002 $e^-/\text{Å}^2$. In this estimation, we are assuming a linear relation between the charge transfer and the number of flat molecules.

B. Effect of charged surfaces: Pd(111)

We have performed two additional AIMD simulations with a positive ($+1|e|$) and negative ($-1|e|$) extra net charge to analyze how the domain order is modified under charged electrode conditions. Each simulation is also 10 ps long. PBE was chosen for XC, and the unit cell is the same as for the neutral case.

As these simulations are performed under periodic boundary conditions, to avoid the divergence of the electrostatic potential due to the extra charge (which will always be located within the metal slab), a compensating neutralizing charge background is uniformly distributed within the unit cell. This set up does not represent a realistic electrochemical cell with an applied bias. It is not our intention in this work to have an accurate correspondence between surface charge (or applied bias) and the exact induced dipole and molecular order at the interface. The aim of these calculations is to obtain an insight on how the water molecules would locally order at the interface under an applied external bias, and which type of interfacial domain would be favored depending on the sign of the applied bias. Considering that the domains are related to the charge transfer, we have chosen to perform the charged simulations only for the PBE functional, which presented a larger charge transfer for the neutral system. The distribution profiles for these charged systems are shown in Figs. 5(a)–5(d). For the system with a positive net charge, we observe the formation of the double peak in both interfaces, similar to the previously described ordered domain. On the other hand, when the system has a negative net charge, the number of molecules at both interfaces with down orientations increases, and the disordered domain is formed at the two interfaces.

TABLE II. Work function Φ (eV) of bare (111) Pd and Au as obtained using different XC potentials. In parenthesis, the experimental work function for the bare (111) surfaces is provided. Averaged work function change ($\Delta\Phi = \Phi_{metal/H_2O} - \Phi_{metal}$) (eV) as obtained from our AIMD simulations. Estimation of net charge transfer (σ_{CT}) from water to the metal interface, in $e^-/\text{Å}^2$.

	XC	Φ (eV)	ΔΦ (eV)	σ_{CT} ($e^-/\text{Å}^2$)
Pd	PBE	5.15 (5.6[42])	1.15 ± 0.44	3.0×10^{-3}
Pd	vdW-DF^{PBE}	5.40	1.22 ± 0.28	1.5×10^{-3}
Au	PBE	5.13 (5.31[42])	−0.58 ± 0.37	8.0×10^{-5}
Au	vdW-DF^{PBE}	5.34	−0.68 ± 0.39	3.0×10^{-5}

C. Au(111) surfaces

Current water/metal interatomic potentials[21,22,36] do not take into account the charge transfer effect which seems to be the origin of the domains. They also are parametrized to reproduce single molecule water absorption geometries, which we have shown do not reproduce the actual interfacial geometry of fully solvated surfaces. However, they describe very accurately the electrostatic interaction between the image charges at the metal and the solvent. To compare our results with a system where water/metal interactions are more electrostatically dominated, due to the absence of charge transfer,[14] we have also performed AIMD simulations (with both PBE and vdW-DF^{PBE} functionals) of the Au(111)-H_2O interface.[37] The z-distribution profiles are shown in Figs. 6(a) and 6(b). Contrary to the Pd-H_2O system, we do not observe a double peak at the interface at any point, indicating that with Au, there are more down/up molecules at the interfaces. This broad distribution of the orientation of the water molecules can be observed in the largest dispersion of the angle distribution, shown in Figs. 4(c) and 4(d), for Au simulations using PBE and vdW-DF^{PBE}, respectively.

Qualitatively, the inclusion of the vdW term affects in a different way the Pd/H_2O system compared to the Au one. In Pd case, there is a very strong binding of the flat molecules due the binding overestimation of PBE.[7] The inclusion of vdW dispersion makes the system more diffusive[34] but does not modify the interfacial domains. Instead, it makes these domains to fluctuate over time, as opposed to the steady domains observed in the PBE simulation, which would fluctuate at a higher simulation temperature (see Fig. 3). However, for Au, we do not observe domains, and the binding at the interface is weaker. What vdW does in this case is to change more the orientation of the water molecules at the interface. This will have an effect in the solvated work function, as will be shown below.

D. Vibrational density of states: Au vs Pd

The vibrational spectra of water can provide information about the hydrophobic nature of the interfaces, given that hydrophobic interfaces are characterized by the presence of dangling, non-H-bonded molecules, with a blue-shifted peak in stretching region of the spectrum.[38] In Fig. 6(c), we show

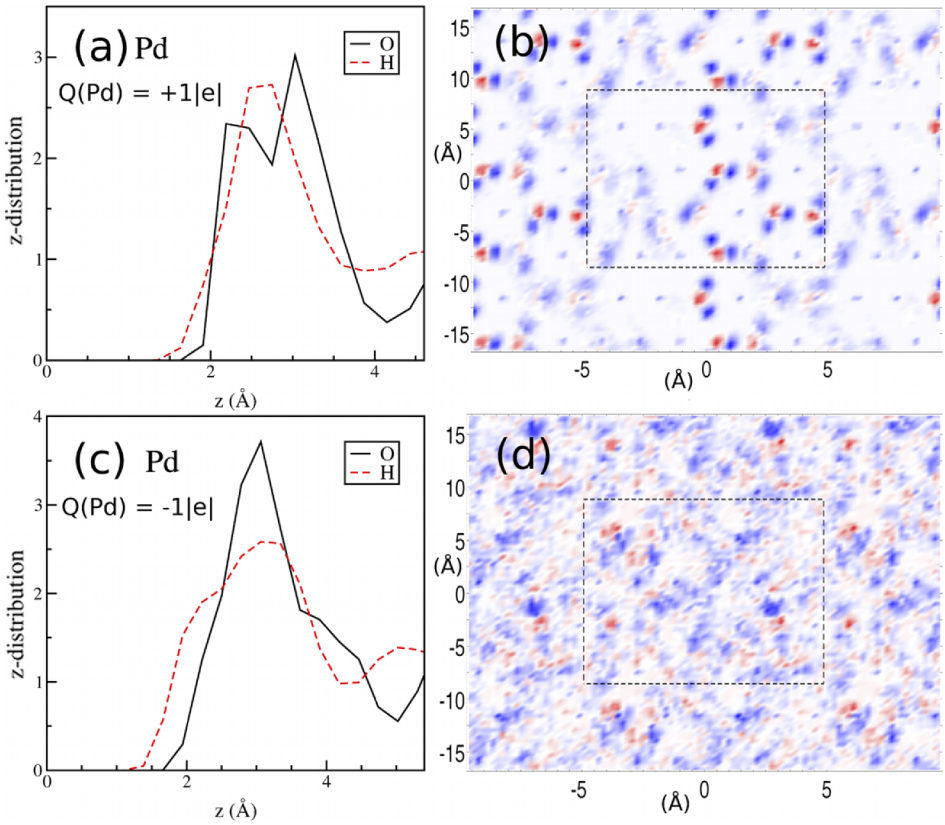

FIG. 5. z-distribution for O and H atoms computed along the z–distance (in Å) at the Pd/H_2O interface for charged simulations with net charge $+1|e|$ in (a) and $-1|e|$ in (c) using PBE XC. Slab surface corresponds to the zero in z. The XY surface probability at the interfaces is shown in (b) for $+1|e|$ and in (d) for $-1|e|$. Water molecules can be seen formed by O (red) and H (blue). The first Pd layer below is shown in small black spots. The square indicates the unit cell used in the AIMD simulations.

the vibrational density of states (DOS), obtained via the Fourier transform of the velocity auto-correlation function, for all water molecules. This dangling OH signature is only weakly present in the Au/PBE simulation. However, we can observe a relative blueshift of the overall stretching peak from Pd to Au indicating that the H-bond network is weakened in water at the interface of Au.[18] This difference between Pd and Au can also be taken as an indication of larger hydrophobicity for Au with

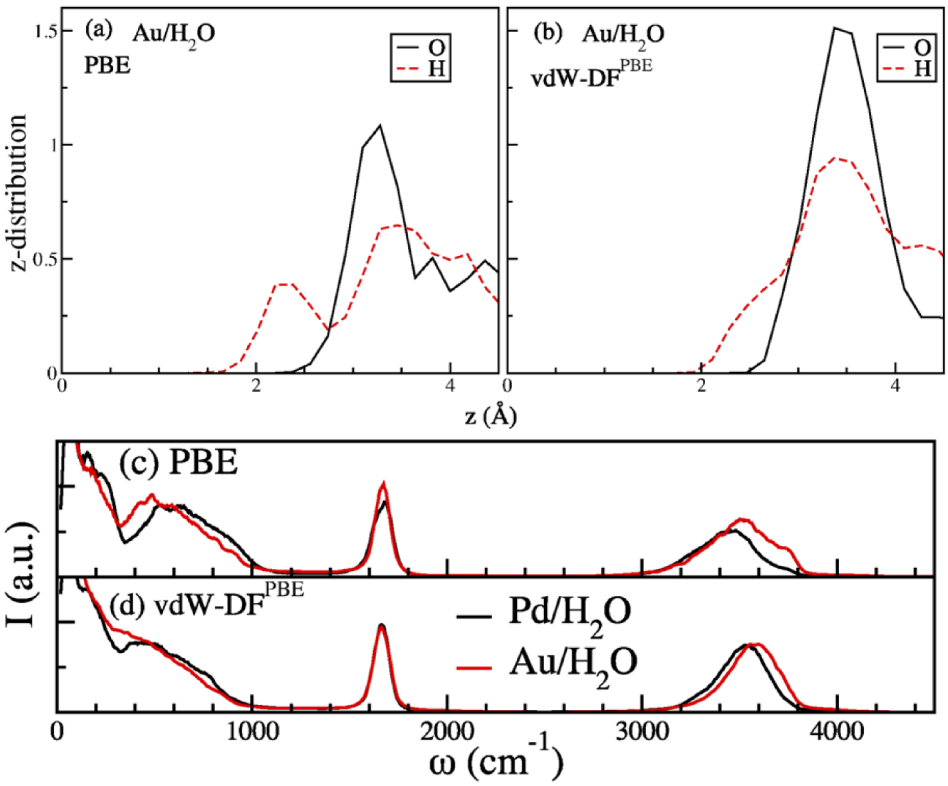

FIG. 6. Top: z-distribution for O and H atoms computed along the z–distance (in Å) at the Au/H_2O interface for (a) PBE and (b) vdW-DF^{PBE}. The surface of the slab is set to zero in the z-axis. Bottom: vibrational density of states for Pd/H_2O (black lines) and Au/H_2O (red lines) as obtained for (c) PBE and (d) vdW-DF^{PBE} simulations.

respect to Pd, which could be considered more hydrophilic than hydrophobic.

E. Solvated work function

Our results with Pd and Au allow us to explore changes in the work function of these metals upon solvation. A standard concept in electrochemistry is the potential of zero charge (PZC). This is the electrode's potential at the so called point of zero charge, which is the state of the pure solvent, free of ions. In principle, this is the same as the work function (Φ) of the solvated electrode.[39] Here, we evaluate change of the work function of the metal upon solvation, $\Delta\Phi = \Phi_{m/H_2O} - \Phi_m$ (m = Au/Pd). When the metal surface is fully solvated, this change does not necessarily need to be the same as the change observed upon gas absorption.[15,39] In the latter case, the change is due to the adsorption of one or very few water monolayers with very specific structures, and in general $\Delta\Phi < 0$, indicating that the dipole of the adsorbed water molecules is antiparallel to the clean surface's dipole (which is always perpendicular to the surface and pointing inwards). Therefore, in those cases, water adsorbs with the oxygen atom facing the surface, as already shown in numerous studies.[4,5,8,9,39] For fully solvated surfaces, obtaining an accurate $\Delta\Phi$ is a challenge both theoretically[15] and experimentally.[39,40]

To compute Φ for the bare surface (Φ_m, m = Au/Pd), we evaluate $\Phi = E_v - E_F$, where E_v is the planar averaged electrostatic potential energy in the near vacuum region next to the bare surface and E_F is the Fermi level of the system. The solvated surface's (Φ_{m/H_2O}, m = Au/Pd) work function is computed in the same way, after correct alignment of the metal's electrostatic potential with that of the bare surface, therefore referencing with respect to the same vacuum level (i.e., to the same arbitrary zero of potential).[41] We computed Φ for representative configurations from the AIMD. In Table II, we show the time-averaged work function change, $\Delta\Phi$ and Φ_m, for both Pd and Au.

The work function of the Pd/H_2O interface increases with respect to the Pd(111) clean surface. The two domains previously described, in-plane ordered and in-plane disordered, have opposed interfacial dipoles. The disordered domain, with a larger number of "down" molecules, has a net negative interfacial dipole moment, i.e., with the dipole vector antiparallel to the vector normal to the surface. This is the reason why the net work function change is positive, indicating that, despite the ordered domain would tend to decrease the work function both because of the charge transfer and "push-back" effect[43] associated to the physisorption of flat molecules, the large interfacial dipole of the disordered domain dominates the sign of the work function change. It is interesting to note that with vdW-DF^{PBE}, the net charge transfer is reduced, which correlates with an increase of the solvated work function, as expected.

For Au, the change in work function is smaller and of opposite sign as compared to Pd. The net interfacial dipole is small, because most of the interfacial water are flat-down or flat-up, therefore canceling each others contribution to the net dipole. Overall, the "push-back" effect[43] dominates and the work function decreases. We observe a negligible amount of charge transfer for Au, as we expected. Overall, our results show that the change in work function upon solvation is strongly metal dependent.

IV. CONCLUSIONS

In conclusion, we have showed how liquid-water interacts with Pd and Au (111) surfaces using AIMD simulations. Our results show that the inclusion of the electronic degrees of freedom (in this case, via DFT) is essential to properly describe the interaction of water and metal surfaces in general. This study has explored two important aspects critical for understanding how to achieve accurate simulations of the electrochemical interface. First of all, we have evaluated the importance of vdW interactions in DFT when simulating liquid water and metallic surfaces. Our results show that accounting for vdW interactions is particularly critical, mostly because of the description of liquid water itself. Second, we have addressed whether the nature of the metallic surface affects the liquid structure at the interface. Our results show that, contrary to what has been claimed using classical potentials,[21] the order of water at the interface strongly depends on the metal under consideration and is not always hydrophobic. In particular, for Pd, we have shown that liquid water adsorbs, forming two different domain structures, which are driven by the strong physisorption of "flat"-type water molecules and associated with charge transfer mechanism. For Au, we do not observe the formation of domains, which is related to the lack of charge transfer at the interface. We have also computed the change of the work function upon solvation of the metal and showed that it is metal dependent, and strongly related to the charge transfer mechanism.

ACKNOWLEDGMENTS

We acknowledge fruitful discussions with Alexandre R. Rocha. This research used computational resources at the Center for Functional Nanomaterials, Brookhaven National Laboratory, which is supported by the U.S. Department of Energy under Contract No. DE-AC02-98CH10886. The work was funded by DOE Early Career Award No. DE-SC0003871.

[1]M. A. Henderson, Surf. Sci. Rep. **46**, 1 (2002).
[2]C. S. Cucinotta, M. Bernasconi, and M. Parrinello, Phys. Rev. Lett. **107**, 206103 (2011).
[3]M. K. Petersen, R. Kumar, H. S. White, and G. A. Voth, J. Phys. Chem. C **116**, 4903 (2012).
[4]A. Michaelides, V. A. Ranea, P. L. de Andres, and D. A. King, Phys. Rev. Lett. **90**, 216102 (2003).
[5]J. Carrasco, A. Michaelides, and M. Scheffler, J. Chem. Phys. **130**, 184707 (2009).
[6]A. Hodgson and S. Haq, Surf. Sci. Rep. **64**, 381 (2009).
[7]A. Poissier, S. Ganeshan, and M. V. Fernandez-Serra, Phys. Chem. Chem. Phys. **13**, 3375 (2011).
[8]T. Mitsui, M. K. Rose, E. Fomin, D. F. Ogletree, and M. Salmeron, Science **297**, 1850 (2002).
[9]J. Cerda, A. Michaelides, M.-L. Bocquet, P. J. Feibelman, T. Mitsui, M. Rose, E. Fomin, and M. Salmeron, Phys. Rev. Lett. **93**, 116101 (2004).
[10]J. Carrasco, J. Klimes, and A. Michaelides, J. Chem. Phys. **138**, 024708 (2013).
[11]A. Michaelides, A. Alavi, and D. King, Phys. Rev. B **69**, 113404 (2004).
[12]M. Tatarkhanov, D. F. Ogletree, F. Rose, T. Mitsui, E. Fomin, S. Maier, M. Rose, J. Cerdá, and M. Salmeron, J. Am. Chem. Soc. **131**, 18425 (2009).

[13]F. McBride, A. Omer, C. M. Clay, L. Cummings, G. R. Darling, and A. Hodgson, J. Phys.: Condens. Matter **24**, 124102 (2012).
[14]S. Schnur and A. Groß, New J. Phys. **11**, 125003 (2009).
[15]S. Duan, X. Xu, Z.-Q. Tian, and Y. Luo, Phys. Rev. B **86**, 045450 (2012).
[16]S. Izvekov, A. Mazzolo, K. VanOpdorp, and G. A. Voth, J. Chem. Phys. **114**, 3248 (2001).
[17]S. Izvekov and G. A. Voth, J. Chem. Phys. **115**, 7196 (2001).
[18]R. Nadler and J. F. Sanz, J. Chem. Phys. **137**, 114709 (2012).
[19]G. Cicero, A. Calzolari, S. Corni, and A. Catellani, J. Phys. Chem. Lett. **2**, 2582 (2011).
[20]K. Letchworth-Weaver and T. A. Arias, Phys. Rev. B **86**, 075140 (2012).
[21]D. T. Limmer, A. P. Willard, P. Madden, and D. Chandler, Proc. Natl. Acad. Sci. U. S. A. **110**, 4200 (2013).
[22]A. P. Willard, D. T. Limmer, P. Madden, and D. Chandler, J. Chem. Phys. **138**, 184702 (2013).
[23]D. T. Limmer, C. Merlet, M. Salanne, D. Chandler, P. A. Madden, R. van Roij, and B. Rotenberg, Phys. Rev. Lett. **111**, 106102 (2013).
[24]J. Carrasco, B. Santra, J. Klimes, and A. Michaelides, Phys. Rev. Lett. **106**, 026101 (2011).
[25]P. Ordejón, E. Artacho, and J. M. Soler, Phys. Rev. B **53**, 10441 (1996).
[26]J. M. Soler, E. Artacho, J. D. Gale, J. J. A. García, P. Ordejón, and D. Sánchez-Portal, J. Phys.: Condens. Matter **14**, 2745 (2002).
[27]J. P. Perdew, K. Burke, and M. Ernzerhof, Phys. Rev. Lett. **77**, 3865 (1996).
[28]M. Dion, H. Rydberg, E. Schroder, D. C. Langreth, and B. I. Lundqvist, Phys. Rev. Lett. **92**, 246401 (2004).
[29]J. Wand, G. Roman-Perez, J. Soler, E. Artacho, and M.-V. Fernandez-Serra, J. Chem. Phys. **134**, 024516 (2011).
[30]F. Corsetti, E. Artacho, J. M. Soler, S. S. Alexandre, and M. V. Fernandez-Serra, J. Chem. Phys. **139**, 194502 (2013).
[31]N. Troullier and J. L. Martins, Phys. Rev. B **43**, 1993 (1991).
[32]M. V. Fernandez-Serra and E. Artacho, J. Chem. Phys. **121**, 11136 (2004).
[33]F. Corsetti, M. V. Fernandez-Serra, J. M. Soler, and E. Artacho, J. Chem. Phys. **139**, 194502 (2013).
[34]As already discussed in other studies,[29,30] dispersion interactions largely increase the room temperature diffusivity of vdW-DF^{PBE} liquid water with respect to PBE.
[35]J.-S. Filhol and M.-L. Doublet, Catal. Today **202**, 87 (2013).
[36]J. I. Siepmann and M. Sprik, J. Chem. Phys. **102**, 511 (1995).
[37]The Au simulations were performed for a 4 layers of 12 atoms (48 in total) with a unit cell in the XY direction half the size of that of Pd, with area = 9.753×9.373 Å and 40 water molecules in total.
[38]G. Cicero, J. C. Grossman, E. Schwegler, F. Gygi, and G. Galli, J. Am. Chem. Soc. **130**, 1871 (2008).
[39]V. Tripkovic, M. E. Björketun, E. Skúlason, and J. Rossmeisl, Phys. Rev. B **84**, 115452 (2011).
[40]F. Musumeci and G. H. Pollack, Chem. Phys. Lett. **536**, 65 (2012).
[41]G. Heimel, L. Romaner, E. Zojer, and J.-L. Bredas, Acc. Chem. Res. **41**, 721 (2008).
[42]H. B. Michaelson, J. Appl. Phys. **48**, 4729 (1977).
[43]S. Braun, W. R. Salaneck, and M. Fahlman, Adv. Mater. **21**, 1450 (2009).